Article

Microbially accelerated carbonate mineral precipitation as a strategy for in situ carbon sequestration and rehabilitation of asbestos mine sites

Jenine McCutcheon, Siobhan Alexandra Wilson, and Gordon Southam

Environ. Sci. Technol., **Just Accepted Manuscript** • DOI: 10.1021/acs.est.5b04293 • Publication Date (Web): 31 Dec 2015

Microbially accelerated carbonate mineral precipitation as a strategy for *in situ* carbon sequestration and rehabilitation of asbestos mine sites

Jenine McCutcheon[1*], *Siobhan A. Wilson*[2], *and Gordon Southam*[1]

[1]School of Earth Sciences, The University of Queensland, St Lucia, QLD 4072, Australia

[2]School of Earth, Atmosphere and Environment, Monash University, Clayton, Melbourne, VIC 3800, Australia

*Corresponding author: School of Earth Sciences, The University of Queensland, St Lucia, QLD 4072, Australia; phone: +61 7 3365 1180, fax: +61 7 3365 1277; j.mccutcheon@uq.edu.au

Prepared for submission to: *Environmental Science & Technology*

Key words: carbon sequestration, asbestos, carbon dioxide, mine site rehabilitation mine tailings, dypingite, carbonate precipitation, air capture

ABSTRACT

A microbially accelerated process for precipitation of carbonate minerals was implemented in a sample of serpentinite mine tailings collected from the abandoned Woodsreef Asbestos Mine in NSW, Australia as a strategy to sequester atmospheric CO_2 while also stabilizing the tailings. Tailings were leached using sulfuric acid in reaction columns and subsequently inoculated with an alkalinity-generating cyanobacteria dominated microbial consortium that was enriched from pit waters at the Woodsreef Mine. Leaching conditions that dissolved 14% of the magnesium from the serpentinite tailings while maintaining circumneutral pH (1800 ppm, pH 6.3) were employed in the experiment. The mineralogy, water chemistry, and microbial colonization of the columns were characterized following the experiment. Micro X-ray diffraction was used to identify carbonate precipitates as dypingite [$Mg_5(CO_3)_4(OH)_2 \cdot 5H_2O$], hydromagnesite [$Mg_5(CO_3)_4(OH)_2 \cdot 4H_2O$], with minor nesquehonite ($MgCO_3 \cdot 3H_2O$). Scanning electron microscopy revealed that carbonate mineral precipitates form directly on the filamentous cyanobacteria. These findings demonstrate the ability of these organisms to generate localized supersaturating microenvironments of high concentrations of adsorbed magnesium and photosynthetically generated carbonate ions, while also acting as nucleation sites for carbonate precipitation. This study is the first step towards implementing *in situ* carbon sequestration in serpentinite mine tailings via microbial carbonate precipitation reactions.

INTRODUCTION

Carbonate mineral precipitation in ultramafic mine tailings is being pursued as a strategy to develop carbon neutral mines (*1*). Mine tailings provide an excellent substrate for carbonate formation because the ore extraction process increases the surface area of the tailing grains,

resulting in higher potential (engineered) weathering and carbonate precipitation rates than those for natural bedrock (Reactions 1 and 2) (*2-7*). Seifritz (*8*) was the first to propose sequestering CO_2 in carbonate minerals, followed by extensive research in passive and active methods for trapping and storing CO_2 within this stable carbon sink (*9-22*).

Microbial photosynthesis is known to accelerate carbonate mineral precipitation by generating an alkaline aqueous environment in which bicarbonate and hydroxyl ions react to produce carbonate ions (Reactions 3 and 4), thereby inducing mineralization (Reaction 2) (*23, 24*). Microbially enabled carbonate formation has been documented for more than a century in many natural and engineered environments (*16, 24-39*). In addition to inducing the necessary chemical setting, microbes also provide nucleation sites for carbonate mineral precipitation (*36, 40, 41*). Previous laboratory experiments have demonstrated the ability of cyanobacteria to utilize atmospheric CO_2 for the precipitation of hydromagnesite [$Mg_5(CO_3)_4(OH)_2 \cdot 4H_2O$] from magnesium-rich solutions similar to those likely to be derived from acid leaching of mine tailings (*24*).

$$Mg_3Si_2O_5(OH)_4 + 3\ H_2SO_4 \rightarrow 3\ Mg^{2+} + 2\ Si(OH)_4 + H_2O + 3\ SO_4^{2-} \quad (1)$$

$$5\ Mg^{2+} + 4\ CO_3^{2-} + 2\ OH^- + 5\ H_2O \rightarrow Mg_5(CO_3)_4(OH)_2 \cdot 5H_2O \quad (2)$$

$$HCO_3^- + H_2O \rightarrow CH_2O + O_2 + OH^- \quad (3)$$

$$HCO_3^- + OH^- \rightarrow CO_3^{2-} + H_2O \quad (4)$$

The tailings produced by ultramafic-hosted mines react naturally with the atmosphere to produce magnesium carbonate minerals; however, there is potential to enhance the rate and scale of this carbonation reaction using stronger acids, such as H_2SO_4, and microbially catalyzed

reactions (*1, 42*). Oskierski, et al. (*43*) identified and characterized naturally occurring carbonate precipitation at the Woodsreef Asbestos Mine, located near Barraba, NSW, Australia. Carbon storage in chrysotile mine tailings such as those found at Woodsreef is desirable because the carbonate precipitation process remediates the hazardous asbestos fibers remaining after the cessation of mining activity (*44*) and assists in establishing slope stability (*14*). The purpose of this investigation is to characterize the ability of a consortium of cyanobacteria naturally present at the Woodsreef Mine to induce precipitation of magnesium carbonate minerals in samples of Woodsreef tailings.

EXPERIMENTAL SECTON

Regional geology and characterization of untreated mine tailings. The Woodsreef Mine is situated in the Great Serpentine Belt (GSB) (267.2 ± 1.4 Ma), which is comprised of partially serpentinized harzburgite, massive serpentinite, and schistose serpentinite (See Supporting Information, SI, for details) (*43, 45, 46*). Mining activity (1971–1983) produced 550 000 t of chrysotile, with the derelict mine site occupying 400 hectares and hosting 75 million t of waste rock, 24.2 million t of tailings, and four 'lakes' in the open pits (pH 8.6–9.0) (Figure 1) (*47, 48*). The Woodsreef tailings are composed of serpentine-group minerals (lizardite and chrysotile) [$Mg_3Si_2O_5(OH)_4$] with minor magnetite (Fe_3O_4), chromite ($FeCr_2O_4$), enstatite ($MgSiO_3$), forsterite (Mg_2SiO_4), calcite ($CaCO_3$), quartz (SiO_2) and brucite [$Mg(OH)_2$] with hydromagnesite [$Mg_5(CO_3)_4(OH)_2{\cdot}4H_2O$] and pyroaurite [$Mg_6Fe_2(CO_3)(OH)_{16}{\cdot}4H_2O$] forming as alteration products (*43, 49*). A Woodsreef tailings sample was examined using scanning electron microscopy (SEM) and analyzed using energy dispersive spectroscopy (EDS), providing a 'time zero' example of the tailings (see SI for details). A sample of the carbonate crusts

(hydromagnesite with minor calcite and dolomite) that are found on vertical surfaces on the tailings pile (*43*) was characterized using SEM-EDS.

Mine tailing leaching trial. A leaching experiment was completed to resolve the ability of the Woodsreef tailings to act as a soluble magnesium source for carbonate precipitation (Equation 1)(*5, 6*). Five leaching experiments were conducted, each containing 5 g of the Woodsreef tailings in 100 mL of dilute sulfuric acid (0.04, 0.08, 0.15, and 0.30 M), with the control experiment containing deionized water. Hereafter, the leaching systems are identified by the molar concentration of sulfuric acid. The flasks were placed on a shaker table operating at 100 rpm. The pH of each flask was measured at time zero, followed by measurements at 4 h, 8 h, 24 h, and then daily for 44 days until the flasks reached steady state, as indicated by a constant pH. Major cation concentrations were measured in a 0.45 μm-filtered sample of water from each system using inductively coupled plasma optical emission spectroscopy (ICP-OES; see SI for details). The remaining tailings were washed with deionized water, dried, and examined using SEM-EDS.

Microbial carbon mineralization experiment. The leaching trial results were used to determine which conditions balanced (1) a high, but not toxic, concentration of soluble magnesium with (2) a pH suitable for the survival and growth of photosynthetic microorganisms. These conditions were used to design the carbon mineralization experiment. Five reaction columns were constructed in syringes (60 cc), each containing 90 g of unconsolidated Woodsreef tailings containing no visible evidence of mineral carbonation. The tailings were leached for 6 weeks with 23 mL of 0.022 M sulfuric acid (pH 1.4), targeting a concentration of 2000 ppm Mg^{2+} in solution. After leaching, one column was air dried and sampled for examination using SEM-EDS. Three columns were inoculated with 2.3 mL of the consortium grown from Lake 4 at the

Woodsreef Mine. The final column was not inoculated to act as a 'tailings control'. These four columns were wrapped with aluminum foil to simulate natural surface light conditions for the microbial phototrophs.

Additional 5 mL (pH 1.8) aliquots of 0.022 M sulfuric acid containing 10% BG-11 growth medium(*50*) were added weekly to the bottom of each of the four columns. After 4 weeks, the top surfaces of the columns and the tailings 2 cm below the surface were sampled for SEM-EDS. Surface samples of all the columns were also collected and air-dried at room temperature for micro X-ray diffraction (μXRD; see SI for details).

Residual pore solution samples could not be directly collected from the columns to examine pore water chemistry following experimentation. A volume of dH_2O equal to 2× the pore volume was added to one of the inoculated columns and to the tailings control to recover readily soluble materials. One pore volume of water was drained from each column for analysis using ICP-OES.

RESULTS

Characterization of untreated mine tailings. Examination of the Woodsreef tailings using SEM-EDS produced results consistent with the mineralogical characterization of Oskierski, et al. (*43*). The tailings consist of aggregates of disseminated chrysotile fibers (~100 nm-scale in diameter, hundreds of μm long) (Figure 2A), and grains of massive serpentinite. The carbonate crusts consist of chrysotile fibers and platy crystals (< 6 μm) of magnesium carbonate minerals that are morphologically similar to those produced in comparable magnesium carbonate precipitation studies (Figure 2B) (*24*). Examination of polished sections of the carbonate crusts

shows serpentinite fragments encased in magnesium carbonate cement (Figure 2C). The crusts contain filamentous microorganisms in close spatial association with the carbonate precipitates.

Mine tailing leaching trial. The buffering capacity of the tailings caused an increase in pH and generation of a high concentration of soluble magnesium (Table 1, SI Figure S1). The control system had a starting pH of 6.9 that increased to between 8.3 and 8.9 for the duration of the experiment, releasing 30 ppm (Mg^{2+}) into solution. Leaching with acid concentrations of 0.04, 0.08, 0.15, and 0.30 M released 1786 ppm, 3407 ppm, 6848 ppm, and 9525 ppm (Mg^{2+}) into solution, respectively (Table 1). Only the 0.04 M system reached a circumneutral pH (final pH of 6.3) suitable for survival of the cyanobacteria, and was therefore used as a guide for the column experiment. Characterization of the leached tailings using SEM-EDS demonstrated that all of the reaction systems contained intact fibers at the conclusion of the leaching experiment (SI Figure S2).

Microbial carbon mineralization experiment. The tailings in the columns contained intact fibres after 6 weeks of leaching with sulfuric acid (SI Figure S3A). After 4 weeks of microbial growth in the inoculated columns, a solid crust, plus mm-scale white mineral grains, formed on the surface of the tailings (Figure 3A). Examination of this crust using SEM-EDS revealed extensive magnesium carbonate precipitation in association with filamentous cyanobacteria (Figure 3B). Rosettes of magnesium carbonate crystals can be observed filling voids within the biofilm (Figure 3C). A ‘mesh’ of extra-cellular polymeric substances (EPS) coats the microbial cells (Figure 3D) and can be seen on and within many of the rosettes (Figure 3E). The white grains visible in Figure 3A appear to be composed of elongated crystals of nesquehonite (Figure 3F). Hollow casts of cells that had become encrusted with magnesium carbonate can be seen throughout the samples (SI Figure S3B).

The complexity of the crusts in the inoculated columns became apparent when viewed in cross-section using backscattered electron imaging (Figures 4 and 5). A microbial biofilm up to 100 μm thick was visible at the interface between the atmosphere and the mineral grains at the surface of the columns (Figure 4A). Magnesium carbonate precipitates were observed nucleating from the surfaces of serpentine grains, cementing them into the crust that was visible macroscopically on the surface of each column inoculated with the mine site microbial consortium (Figure 4B). This magnesium carbonate cement commonly exhibited evidence of microbial casts or 'fossils' (Figure 5A); however, these were not ubiquitous throughout the samples (Figure 5B).

In contrast, the control column did not produce a consolidated crust, and therefore was not embedded for thin section preparation. When viewed as a whole mount using SEM-EDS, samples from the control column exhibited some magnesium carbonate precipitates; however, they were far less abundant than those in the inoculated columns (SI Figure S3C). Chrysotile, pyroaurite, and dypingite that had dehydrated partly to hydromagnesite were identified using μXRD (SI Figure S4A). μXRD of the surfaces of the inoculated columns identified chrysotile, dypingite, and partially dehydrated hydromagnesite (SI Figure S4B), and confirmed that the crystals shown in Figure 3E are composed of nesquehonite (SI Figure S4C). ICP-OES analysis of the water washed through the inoculated and tailings control columns revealed a decrease in the soluble Mg concentration from an initial high of ~1786 ppm to post-experiment values of 397 ppm and 449 ppm, respectively, suggesting that much of the Mg leached from the tailings was consumed by magnesium carbonate precipitation (Table 2).

DISCUSSION

Chrysotile dissolution. A stoichiometric calculation of the theoretical amount of magnesium that should be produced by each of these acid concentrations indicates that slightly more magnesium was leached than expected (SI Figure S5), a phenomenon observed by McCutcheon, et al. (*51*). The observed non-stoichiometric dissolution is likely due to preferential dissolution of the brucite (Mg-rich) layers over the siloxane (Si-rich) layers in serpentine minerals (*5*). Dissolution of the brucite-like layers is more favorable because the energy required to remove silica from the crystal structures of serpentine minerals is higher than that needed for magnesium (*52-55*). This characteristic of serpentine dissolution also explains why less than 1% of the silica in the tailings was dissolved, and all of leaching systems had Si concentrations at least two orders of magnitude lower than those of Mg (Table 1).

Biologically-mediated versus abiotic carbonate mineral nucleation. The inoculated columns produced hydrated magnesium carbonate precipitates (dypingite, hydromagnesite, and nesquehonite) in close association with extensive growth of filamentous cyanobacteria (Figure 3). The combination of microbial biofilm and mineral precipitate generated a consolidated crust, effectively demonstrating the ability these organisms to generate microenvironments of carbonate supersaturation (*24*). In contrast, the dypingite precipitation observed in the control column was not sufficient to generate a laterally extensive crust, failing to consolidate the tailings. This difference highlights the important role cyanobacteria can play in carbonate mineral nucleation through the attraction of soluble magnesium to the negatively charged cell exteriors and extracellular polymeric substances (EPS) produced by cyanobacteria (*56*). Adsorption of magnesium to microbial surfaces and EPS disrupts the strong hydration shell of six octahedrally coordinated water molecules that typically surrounds each magnesium ion in solution, initiating magnesium carbonate mineral nucleation and growth by increasing the

interaction between magnesium and carbonate ions (*57, 58*). The challenge of completely stripping magnesium ions of water represents a considerable kinetic hurdle to carbonate mineral precipitation, demonstrated by the difficulty of forming magnesite ($MgCO_3$) at Earth surface conditions (*59*). The hydrated magnesium carbonate phases formed in the present study are a product of this kinetic inhibition.

Although the casts (Figure 3E, SI Figure S3B) and 'fossils' (Figure 5A) of filamentous cyanobacteria in the carbonate minerals demonstrate the close relationship between the microbial cells and the mineral precipitates, some regions of the crust were devoid of these features (Figure 5B). The lack of microbial casts in some regions may result from the destruction of cell remnants and associated casts during growth of carbonate crystals, or they may suggest a combination of biological and abiotic carbonate mineral precipitation. For instance, once the hurdle of mineral nucleation has been overcome, either on microbial cells or on serpentinite grains (Figure 5B), abiotic processes may then be sufficient to continue carbonate crystal growth. Alternatively, these carbonate precipitates may have nucleated on the extensive EPS generated by the cyanobacteria, rather than on the cells. In this case, the fluid, labile nature of EPS would prevent its preservation during crystal growth, resulting in what appears to be abiotic carbonate precipitation.

The precipitation of nesquehonite in the inoculated columns, and the dypingite in both the inoculated and control columns, is likely the result of dissolution of atmospheric CO_2 combined with evapoconcentration of magnesium within the air–water boundary at the surface of the columns (*60, 61*). The carbonate precipitation observed in the inoculated columns was more extensive than that in the control column, indicating that evapoconcentration combined with the photosynthetic activity of cyanobacteria is more effective than evapoconcentration alone. The

pyroaurite identified in the control column may have been present in the tailings prior to the experiment, as pyroaurite can account for up to 5 wt% of the surface tailings at Woodsreef. Alternatively, the pyroaurite may have formed during the carbonation experiment, a possibility supported by the fact that any pre-existing pyroaurite would have dissolved during the leaching step. In this case, some of the soluble magnesium produced in the tailings control column would have been consumed by pyroaurite precipitation, decreasing the amount of CO_2 storage in the tailings control. The lack of pyroaurite and the formation of only carbonate mineral phases in the inoculated columns suggest that the microbial biofilm on the surface of the columns provided ideal geochemical conditions, specifically enhanced carbon availability, for carbonate mineral precipitation.

Mine site rehabilitation. Consolidation of the surface of the Woodsreef Mine tailings pile by with a magnesium carbonate crust, or 'magcrete', would reduce the environmental and human health hazard posed by the asbestos tailings (*44*). *In situ* cementation of the tailings would limit transport of the fibrous asbestos offsite by wind and water. In addition to containing the tailings within the pile, the microbial activity associated with magcrete formation would introduce organic carbon into the tailings, a critical step in rudimentary soil development (*62, 63*). Growth of a mature microbial community in the surficial tailings would initiate the nutrient (N and P) cycling processes necessary prior to the introduction of vegetation and other complex organisms. The microbial biomass would also increase the ability of the tailings to retain water, an important ecological benefit in the arid setting of the Woodsreef Mine.

Mine-scale carbon sequestration. In addition to facilitating mine site rehabilitation, magnesium carbonate formation at the Woodsreef Mine would sequester atmospheric CO_2. Using the targeted magnesium concentration for the 0.04 M leaching system (Table 1) and the post-

carbonate precipitation concentration measured from the columns (Table 2), the amount of CO_2 stored in each of the columns was estimated (Table 3). The inoculated columns saw a decrease in magnesium concentration from the leached value of 1786 ppm to 397 ppm, whereas the magnesium concentration in the tailings control declined to 449 ppm. The values given in Table 3 reflect a simplified scenario, which provides an estimate of the proportion of CO_2 stored per unit area for the inoculated column (dypingite only), the inoculated column (dypingite and biomass), and the tailings control column (pyroaurite) were 137, 478, and 27 g/m^2, respectively. If this proportion of serpentine leaching and carbonate precipitation were implemented on the scale of the Woodsreef tailings pile (0.5 km^2 in area) (*43*) the total mass of CO_2 sequestered would be 69, 239, and 13.5 t for each of these respective scenarios. These biogenic CO_2 storage quantities, achieved in only 4 weeks, are far greater than the background rate of 47 t/year of natural storage occurring in surface hydromagnesite crusts estimated by Oskierski, et al. (*43*).

Although carbon storage in biomass lacks the longevity of storage within minerals, it is still worthy of consideration due to its ability to draw down atmospheric CO_2, promote mineral carbonation (17), and begin the generation of organic carbon necessary for soil development, as previously discussed. Storage in biomass was incorporated into the calculation using the ten cycles of carbon fixation (cyanobacterial photosynthesis) required to produce the four carbonate anions from atmospheric carbon dioxide and two hydroxyls per molecule of dypingite, see McCutcheon, et al. (*24*). The benefit provided by the microbial inoculum is especially evident when the possibility of abiotic pyroaurite production is considered because the higher molar proportion of Mg to CO_2 within this phase limits the amount of CO_2 that can be stored in the tailings.

271 The present study provides a successful first step towards the *in situ* stabilization of
272 chrysotile mine waste by employing a microbial carbon sequestration strategy that uses
273 atmospheric CO_2 as a carbon source. Scaling up to field-based implementation of this process by
274 leaching the top 1 m of the tailings pile and achieving the same proportion of carbonate
275 precipitation as in the column experiment would result in over 2600 t of CO_2 being sequestered
276 in a surface crust within a few weeks. Leaching and reacting this volume of tailings will be
277 challenging considering the arid environment in which Woodsreef is found. Harrison, et al. (*64*)
278 demonstrated that a lack of water inhibited the precipitation of hydrated magnesium carbonate
279 minerals, which may make microbially mediated carbonate precipitation more difficult at the
280 mine site, as aridity would impede both carbonation and microbial activity. The presence of
281 minor dypingite formation in the tailings control column suggests that some CO_2 sequestration
282 will likely occur abiotically following leaching with sulfuric acid. In this case, carbonation
283 would be driven primarily by evapoconcentration of magnesium at the surface of the tailings
284 pile. Assuming that the abiotic rate of carbonate precipitation at Woodsreef would be comparable
285 to that observed in the tailings control columns it could be enhanced by injection of CO_2 into the
286 tailings pile, enabling carbonate precipitation at depth (*15*). The lack of a local point source of
287 CO_2 and the financial and carbon cost associated with transporting CO_2 makes this strategy
288 impracticable for Woodsreef, though this could be a viable option for similar mines located
289 closer to industrial and population centers.

290 The ideal strategy for implementing extensive microbially mediated carbonate
291 precipitation at the Woodsreef Mine would involve directing leached magnesium into a large-
292 scale bioreactor similar to the one utilized in McCutcheon, et al. (*24*). Such a strategy would be
293 applicable to mining operations for which containment of hazardous tailings is not a concern,

294 such as nickel and diamond mines (*65-67*). These 'carbonation ponds' would provide all of the
295 components necessary for successful microbially mediated carbonate precipitation reactions:
296 soluble magnesium leached from the tailings; an environment suitable for the growth of
297 cyanobacteria mats that generate alkalinity and provide carbonate mineral nucleation sites;
298 availability of water for hydrated carbonate mineral formation; and a large 'air-water contact
299 surface area' to 'water volume' ratio to aid atmospheric CO_2 dissolution. Designs for such
300 bioreactors have been proposed previously, such as the 'enhanced passive carbonation plus
301 bioreactor' concept presented by Power, et al. (*1*) for the Mount Keith Nickel Mine. This design
302 utilizes all of the benefits of microbially accelerated carbonate precipitation outlined in the
303 present study, with the added value of biofuel production from biomass harvested from microbial
304 mats(*68*). Ideally, this strategy of carbon storage would employ cyanobacteria found naturally at
305 the site, as these organisms can be found in most circumneutral to alkaline environments (*26-31,*
306 *37*). Using the mineral carbonation rate achieved by McCutcheon, et al. (*24*) for largest lake at
307 Woodsreef (Lake 1; ~12 ha; Figure 1A), the carbon sequestration potential of this lake is ca.
308 1470 t CO_2/year. While this absolute value is substantially smaller than that of a large mine such
309 as Mount Keith (39,800 t CO_2 per year over ~1590 ha) (*1, 42, 61*), the potential rate of CO_2
310 sequestration per unit area is approximately 5 × greater than Mount Keith, and therefore worthy
311 of further study as an integrated small footprint mineral carbonation – biodiesel production
312 process.
313

314 **ACKNOWLEDGEMENTS**

315 We acknowledge the support of grants from Carbon Management Canada and the New South
316 Wales Department of Industry to S.A.W. and G.S. Student support was provided to J.M. by a

Natural Science and Engineering Research Council of Canada (NSERC) Post Graduate Scholarship. We thank J. Hamilton and C. Turvey (Monash University) for their assistance with fieldwork. We thank K. Maddison, N. Staheyeff, C. Karpiel and B. Mullard of NSW Department of Industry for their support of our work at Woodsreef, with particular thanks to K.M., Project Manager for Woodsreef, for her knowledgeable advice. For their technical assistance, we thank Dr. T. Simpson and T. Goldhawk of the Western Nano-fabrication Facility (SEM-EDS), Dr. R. Flemming of Western University (μXRD), and M. Mostert of the Environmental Analytical and Geochemistry Unit at The University of Queensland (ICP-OES).

ASSOCIATED CONTENT

Supporting Information

Analytical technique details and additional results can be found in the Supporting Information. This information is available free of charge via the Internet at http://pubs.acs.org.

Figure 1. A) Aerial view of the Woodsreef Mine tailings pile and pit 'lakes' (labeled) near Barraba, NSW(*69*). B) The tailings primarily consist of unconsolidated, fine-grained serpentine fibers below a layer of pebble-sized serpentine clasts (C). D) Carbonate crusts cover many of the vertical faces on the tailings pile, and help to cement and retain chrysotile fibers. E) The oligotrophic pit waters host microbial communities dominated by phototrophic bacteria.

Figure 2. SEM micrographs of A) fibrous chrysotile in the Woodsreef tailings; B) platelets of a magnesium carbonate mineral among the chrysotile fibers in the tailings; and C) a polished

339 section of a carbonate crust showing the formation of a carbonate cement between the tailings
340 minerals.
341
342 Figure 3. A) Subaerial surface of one of the low acid, inoculated columns containing
343 cyanobacteria (green) and visible grains of magnesium carbonate (white grains). Scanning
344 electron micrographs of: B) filamentous cyanobacteria cells on the surface of the inoculated
345 columns covered in carbonate precipitates; C) the magnesium carbonate crust found coating the
346 cyanobacterial mat in the inoculated columns with a spectrum produced by EDS analysis of the
347 crust (overlay); D) filamentous cyanobacteria connected with a 'mesh' of EPS, all of which is
348 coated in a fine-grained magnesium carbonate precipitate; E) a rosette of magnesium carbonate,
349 likely hydromagnesite or dypingite encrusting a cyanobacterium and minor EPS; and F) acicular
350 crystals within one of the macroscopic magnesium carbonate grains, morphologically and
351 chemically consistent with being nesquehonite, found on the surface of the microbial mats.
352
353 Figure 4. Back-scattered electron micrographs of polished thin sections of the surface of the
354 inoculated columns in cross-section, showing A) a 100 μm thick biofilm of filamentous
355 cyanobacteria (outlined by dotted lines) covering partially cemented serpentine grains; and B)
356 extensive precipitation of magnesium carbonate, which can be seen cementing serpentine grains.
357
358 Figure 5. Back-scattered electron micrographs of polished thin sections of the surface of the
359 inoculated columns in cross-section, showing A) magnesium carbonate cement containing casts
360 of filamentous cyanobacteria; and B) magnesium carbonate cement nucleating from serpentine
361 grains lacking biological features.

362 Table 1. Concentrations (ppm) of major cations in solution for the five systems in the leaching experiment.

			Ion concentration (ppm)										
H_2SO_4 concentration (M)	Initial pH	Final pH	Al	As	Ba	Ca	Cd	Co	Cr	Cu	Fe	K	Mg
0 (H_2O)	6.92	8.29	<DL	<DL	<DL	57.2	<DL	<DL	<DL	<DL	<DL	<DL	30.3
0.04	1.58	6.27	<DL	<DL	<DL	139	<DL	<DL	<DL	<DL	<DL	<DL	1786
0.08	1.30	5.40	<DL	<DL	<DL	210	<DL	<DL	<DL	<DL	<DL	<DL	3407
0.15	0.00	3.41	<DL	<DL	<DL	158	<DL	<DL	24.3	<DL	345	<DL	6848
0.30	0.00	1.72	94.1	<DL	<DL	149	<DL	<DL	0.500	<DL	10.6	<DL	9525

	Ion concentration (ppm)											
Leaching System	Mn	Na	Ni	P	Pb	S	Se	Si	Sr	Ti	V	Zn
0 (H_2O)	<DL	<DL	<DL	<DL	<DL	66.7	<DL	<DL	<DL	<DL	<DL	<DL
0.04	8.32	<DL	22.3	<DL	<DL	1760	<DL	<DL	<DL	<DL	<DL	<DL
0.08	22.5	<DL	83.7	<DL	<DL	3402	0.082	0.608	<DL	<DL	<DL	<DL
0.15	31.9	<DL	110	<DL	<DL	6697	13.2	67.3	<DL	<DL	8.13	<DL
0.30	31.0	<DL	95.6	<DL	<DL	10638	16.7	63.1	<DL	<DL	10.9	<DL

363 <DL: below detection limit

Table 2. Concentrations (ppm) of major cations in solution for the pore waters washed from the columns.

	Ion concentration (ppm)									
Samples	Al	Ca	Fe	K	Mg	Mn	Na	P	Si	Ti
Inoculated column	<DL	27.0	<DL	7.5	397.0	0.0	30.0	<DL	41.3	<DL
Tailings control column	<DL	31.3	<DL	2.9	449.0	0.0	26.9	<DL	44.6	<DL

Table 3. Quantification of CO_2 storage in the experimental columns and potential for storage at Woodsreef Asbestos Mine.

	Columns	Woodsreef Mine	
Sample	Mass of CO_2 stored/area (g/m^2)	Total CO_2 storage at experimental rate (t)	Potential CO_2 storage at leaching depth of 1 m (t)
Inoculated column: dypingite	137	68	759
Inoculated column: dypingite + biomass	478	239	2656
Tailings control column: pyroaurite	27	13.5	149

References

1. Power, I.; McCutcheon, J.; Harrison, A.; Wilson, S.; Dipple, G.; Kelly, S.; Southam, C.; Southam, G., Strategizing carbon-neutral mines: A case for pilot projects. *Minerals* **2014,** *4*, (2), 399-436.
2. White, A. F.; Blum, A. E.; Schulz, M. S.; Bullen, T. D.; Harden, J. W.; Peterson, M. L., Chemical weathering rates of a soil chronosequence on granitic alluvium .1. Quantification of mineralogical and surface area changes and calculation of primary silicate reaction rates. *Geochimica et Cosmochimica Acta* **1996,** *60*, (14), 2533-2550.
3. Molson, J. W.; Fala, O.; Aubertin, M.; Bussiere, B., Numerical simulations of pyrite oxidation and acid mine drainage in unsaturated waste rock piles. *Journal of Contaminant Hydrology* **2005,** *78*, (4), 343-371.
4. Park, A. H. A.; Jadhav, R.; Fan, L. S., CO_2 mineral sequestration: Chemically enhanced aqueous carbonation of serpentine. *Canadian Journal of Chemical Engineering* **2003,** *81*, (3-4), 885-890.
5. Park, A.-H. A.; Fan, L.-S., CO_2 mineral sequestration: Physically activated dissolution of serpentine and pH swing process. *Chemical Engineering Science* **2004,** *59*, 5241-5247.
6. Stumm, W., Chemistry of the solid-water interface. In Wiley-Interscience Publication: New York, 1992; pp 523-598.
7. Wilson, S. A.; Dipple, G. M.; Power, I. M.; Thom, J. M.; Anderson, R. G.; Raudsepp, M.; Gabite, J. E.; Southam, G., Carbon dioxide fixation within mine wastes of ultramafic-hosted ore deposits: examples from the Clinton Creek and Cassiar chrysotile deposits, Canada. *Economic Geology* **2009,** *104*, 95-112.
8. Seifritz, W., CO_2 disposal by means of silicates. *Nature* **1990,** *345*, 486.

9. Bea, S. A.; Wilson, S. A.; Mayer, K. U.; Dipple, G. M.; Power, I. M.; Gamazo, P., Reactive transport modeling of natural carbon sequestration in ultramafic mine tailings. *Vadose Zone Journal* **2012,** *11*, (2).
10. Köhler, P.; Hartmann, J.; Wolf-Gladrow, D. A., Geoengineering potential of artificially enhanced silicate weathering of olivine. *Proceedings of the National Academy of Sciences of the United States of America* **2010,** *107*, (47), 20228-20233.
11. Gerdemann, S. J.; O'Connor, W. K.; Dahlin, D. C.; Penner, L. R.; Rush, H., Ex situ aqueous mineral carbonation. *Environmental Science & Technology* **2007,** *41*, 2587-2593.
12. Power, I. M.; Dipple, G. M.; and Southam, G., Bioleaching of ultramafic tailings by *Acidithiobacillus* spp. for CO_2 sequestration. *Environmental Science & Technology* **2010,** *44*, 456-462.
13. Hansen, L. D.; Dipple, G. M.; Gordon, T. M.; Kellett, D. A., Carbonated serpentinite (listwanite) at Atlin, British Columbia: A geological analogue to carbon dioxide sequestration. *Canadian Mineralogist* **2005,** *43*, 225-239.
14. Wilson, S. A.; Raudsepp, M.; Dipple, G. M., Verifying and quantifying carbon fixation in minerals from serpentine-rich mine tailings using the Rietveld method with X-ray powder diffraction data. *American Mineralogist* **2006,** *91*, 1331-1341.
15. Harrison, A. L.; Power, I. M.; Dipple, G. M., Accelerated carbonation of brucite in mine tailings for carbon sequestration. *Environmental Science & Technology* **2013,** *47*, (1), 126-134.
16. Power, I. M.; Wilson, S. A.; Small, D. P.; Dipple, G. M.; Wan, W.; Southam, G., Microbially mediated mineral carbonation: Roles of phototrophy and heterotrophy. *Environmental Science & Technology* **2011,** *45*, 9061-9068.
17. Lackner, K. S.; Wendt, C. H.; Butt, D. P.; Joyce, E. L.; Sharp, D. H., Carbon-dioxide disposal in carbonate minerals. *Energy* **1995,** *20*, (11), 1153-1170.
18. Schuiling, R. D.; Krijgsman, P., Enhanced weathering: An effective and cheap tool to sequester CO_2. *Climatic Change* **2006,** *74*, (1-3), 349-354.
19. Washbourne, C. L.; Renforth, P.; Manning, D. A. C., Investigating carbonate formation in urban soils as a method for capture and storage of atmospheric carbon. *Science of the Total Environment* **2012,** *431*, 166-175.
20. Renforth, P., The potential of enhanced weathering in the UK. *International Journal of Greenhouse Gas Control* **2012,** *10*, 229-243.
21. Renforth, P.; Manning, D. A. C., Laboratory carbonation of artificial silicate gels enhanced by citrate: Implications for engineered pedogenic carbonate formation. *International Journal of Greenhouse Gas Control* **2011,** *5*, (6), 1578-1586.
22. Krevor, S. C. M.; Lackner, K. S., Enhancing serpentine dissolution kinetics for mineral carbon dioxide sequestration. *International Journal of Greenhouse Gas Control* **2011,** *5*, 1073-1080.
23. Power, I. M.; Wilson, S. A.; Thom, J. M.; Dipple, G. M.; Southam, G., Biologically induced mineralization of dypingite by cyanobacteria from an alkaline wetland near Atlin, British Columbia, Canada. *Geochemical Transactions* **2007,** *8*, (13).
24. McCutcheon, J.; Power, I. M.; Harrison, A. L.; Dipple, G. M.; Southam, G., A greenhouse-scale photosynthetic microbial bioreactor for carbon sequestration in magnesium carbonate minerals. *Environmental Science & Technology* **2014,** *48*, (16), 9142-9151.
25. Drew, G. H., On the precipitation of calcium carbonate in the sea by marine bacteria, and on the action of denitrifying bacteria in tropical and temperate seas. *Journal of Marine Biology Association UK* **1913,** *9*, 479-524.

26. Thompson, J. B.; Ferris, F. G., Cyanobacterial precipitation of gypsum, calcite, and magnesite from natural alkaline water. *Geology* **1990,** *18*, 995-998.
27. Riding, R., Microbial carbonates: the geological record of calcified bacterial-algal mats and biofilms. *Sedimentology* **2000,** *47*, 179-214.
28. Riding, R., Cyanobacterial calcification, carbon dioxide concentrating mechanisms, and Proterozoic-Cambrian changes in atmospheric composition. **2006,** *4*, 299-316.
29. Aloisi, G., The calcium carbonate saturation state in cyanobacterial mats throughout Earth's history. *Geochimica et Cosmochimica Acta* **2008,** *72*, 6037-6060.
30. Ferrer, M. R.; Quevedosarmiento, J.; Rivadenevra, M. A.; Bejar, V.; Delgado, R.; Ramoscormenzana, A., Calcium-carbonate precipitation by 2 groups of moderately halophilic microorganisms at different temperatures and salt concentrations. *Current Microbiology* **1988,** *17*, (4), 221-227.
31. Rivadeneyra, M. A.; Delgado, R.; Delgado, G.; Delmoral, A.; Ferrer, M. R.; Ramoscormenzana, A., Precipitation of carbonates by *Bacillus* sp. isolated from saline soils. *Geomicrobiology Journal* **1993,** *11*, (3-4), 175-184.
32. Boquet, E.; Boronat, A.; Ramoscor.A, Production of calcite (calcium-carbonate) crystals by soil bacteria is a general phenomenon. *Nature* **1973,** *246*, (5434), 527-529.
33. Krumbein, W. E.; Giele, C., Calcification in coccoid cyanobacterium associated with the formation of desert stromatolites. *Sedimentology* **1979,** *26*, (4), 593-604.
34. Merz, M., The biology of carbonate precipitation by cyanobacteria. *Facies* **1992,** *26*, 81-102.
35. Kranz, S. A.; Wolf-Gladrow, D.; Nehrke, G.; Langer, G.; Rost, B., Calcium carbonate precipitation induced by the growth of the marine cyanobacterium *Trichodesmium*. *Limnology and Oceanography* **2010,** *55*, 2563-2569.
36. Pentecost, A.; Bauld, J., Nucleation of calcite on the sheaths of cyanobacteria using a simple diffusion cell. *Geomicrobiology Journal* **1988,** *6*, (2), 129-135.
37. Renaut, R. W., Morphology, distribution, and preservation potential of microbial mats in the hydromagnesite-magnesite playas of the Cariboo Plateau, British Columbia, Canada. *Hydrobiologia* **1993,** *267*, 75-98.
38. Shirokova, L. S.; Mavromatis, V.; Bundeleva, I. A.; Pokrovsky, O. S.; Benezeth, P.; Gerard, E.; Pearce, C. R.; Oelkers, E. H., Using Mg isotopes to trace cyanobacterially mediated magnesium carbonate precipitation in alkaline lakes. *Aquatic Geochemistry* **2013,** *19*, (1), 1-24.
39. Power, I. M.; Wilson, S. A.; Dipple, G. M.; Southam, G., Modern carbonate microbialites from an asbestos open pit pond, Yukon, Canada. *Geobiology* **2011,** *9*, 180-195.
40. Obst, M.; Dynes, J. J.; Lawrence, J. R.; Swerhone, G. D. W.; Benzerara, K.; Karunakaran, C.; Kaznatcheev, K.; Tyliszczak, T.; Hitchock, A. P., Precipitation of amorphous $CaCO_3$ (aragonite-like) by cyanobacteria: A STXM study of the influence of EPS on the nucleation process. *Geochimica et Cosmochimica Acta* **2009,** *72*, 4180-4198.
41. Obst, M.; Wehrli, B.; Dittrich, M., $CaCO_3$ nucleation by cyanobacteria: Laboratory evidence for a passive, surface-induced mechanism. *Geobiology* **2009,** *7*, 324-347.
42. Wilson, S. A.; Harrison, A. L.; Dipple, G. M.; Power, I. M.; Barker, S. L. L.; Ulrich Mayer, K.; Fallon, S. J.; Raudsepp, M.; Southam, G., Offsetting of CO_2 emissions by air capture in mine tailings at the Mount Keith Nickel Mine, Western Australia: Rates, controls and prospects for carbon neutral mining. *International Journal of Greenhouse Gas Control* **2014,** *25*, 121-140.

43. Oskierski, H. C.; Dlugogorski, B. Z.; Jacobsen, G., Sequestration of atmospheric CO_2 in chrysotile mine tailings of the Woodsreef Asbestos Mine, Australia: Quantitative mineralogy, isotopic fingerprinting and carbonation rates. *Chemical Geology* **2013,** *358*, 156-169.
44. Pronost, J.; Beaudoin, G.; Lemieux, J.-M.; Hébert, R.; Constantin, M.; Marcouiller, S.; Klein, M.; Duchesne, J.; Molson, J. W.; Larchi, F.; Maldague, X., CO_2-depleted warm air venting from chrysotile milling waste (Thetford Mines, Canada): Evidence for in-situ carbon capture from the atmosphere. *Geology* **2012,** *40*, 275-278.
45. Glen, R. A.; Butt, B. C., Chrysotile asbestos at Woodsreef, New South Wales. *Economic Geology* **1981,** *76*, (5), 1153-1169.
46. Cawood, P. A.; Pisarevsky, S. A.; Leitch, E. C., Unraveling the New England orocline, east Gondwana accretionary margin. *Tectonics* **2011,** *30*, (5), TC5002.
47. NSW Government Trade & Investment Woodsreef Mine Major Rehabilitation Project. http://www.resourcesandenergy.nsw.gov.au/miners-and-explorers/programs-and-initiatives/derelict/woodsreef-mine-major-rehabilitation-project (30-07-2014),
48. Brown, R. E.; Brownlow, J. W.; Krynen, J. P., Manilla–Narrabri 1:250 000 metallogenic map SH/56-9, SH/55-12: Metallogenic study and mineral deposit data sheets. In Wales, G. S. o. N. S., Ed. New South Wales Department of Mineral Resources: Sydney, 1992.
49. Turvey, C. C. Using a portable X-ray diffractometer for field based carbon accounting at Woodsreef Chrysotile Mine, New South Wales, Australia. Monash University, Clayton, Melbourne, VIC, Australia, 2013.
50. Vonshak, A., Laboratory techniques for the cultivation of microalgae. In *CRC handbook of microalgae mass culture*, Richmond, A., Ed. CRC Press Inc.: Bocca Raton, 1986; p 117.
51. McCutcheon, J.; Dipple, G. M.; Wilson, S. A.; Southam, G., Production of magnesium-rich solutions by acid leaching of chrysotile: A precursor to field-scale deployment of microbially enabled carbonate mineral precipitation. *Chemical Geology* **2015,** *413*, 119-131.
52. Gronow, J. R., The dissolution of asbestos fibres in water. *Clay Minerals* **1987,** *22*, 21-35.
53. Wang, L.; Lu, A.; Wang, C.; Zheng, X.; Zhao, D.; R., L., Nano-fibriform production of silica from natural chrysotile. *Journal of Colloid and Interface Science* **2006,** *295*, 436-439.
54. Morgan, A., Acid leaching studies of chrysotile asbestos from mines in the Coalinga region of California and from Quebec and British Columbia. *Annals of Occupational Hygiene* **1997,** *41*, (3), 249-268.
55. Rozalen, M.; Huertas, F. J., Comparative effect of chrysotile leaching in nitric, sulfuric and oxalic acids at room temperature. *Chemical Geology* **2013,** *352*, 134-142.
56. Beveridge, T. J., The bacterial surface: General considerations towards design and function. *Canadian Journal of Microbiology* **1988,** *34*, (4), 363-372.
57. Kluge, S.; Weston, J., Can a hydroxide ligand trigger a change in the coordination number of magnesium ions in biological systems? *Biochemistry* **2005,** *44*, (12), 4877-4885.
58. Hänchen, M.; Prigiobbe, V.; Baciocchi, R.; Mazzotti, M., Precipitation in the Mg-carbonate system - effects of temperature and CO_2 pressure. *Chemical Engineering Science* **2008,** *63*, 1012-1028.
59. Saldi, G. D.; Jordan, G.; Schott, J.; Oelkers, E. H., Magnesite growth rates as a function of temperature and saturation state. *Geochimica et Cosmochimica Acta* **2009,** *73*, 5646-5657.
60. Power, I. M.; Wilson, S. A.; Dipple, G. M., Serpentinite carbonation for CO_2 sequestration. *Elements* **2013,** *9*, (2), 115-121.

529 61. Power, I. M.; Harrison, A. L.; Dipple, G. M.; Wilson, S. A.; Kelemen, P. B.; Hitch, M.;
530 Southam, G., Carbon mineralization: From natural analogues to engineered systems. *Reviews in*
531 *Mineralogy and Geochemistry* **2013,** *77*, (1), 305-360.
532 62. Šourková, M.; Frouz, J.; Fettweis, U.; Bens, O.; Hüttl, R. F.; Šantrůčková, H., Soil
533 development and properties of microbial biomass succession in reclaimed post mining sites near
534 Sokolov (Czech Republic) and near Cottbus (Germany). *Geoderma* **2005,** *129*, (1–2), 73-80.
535 63. Frouz, J.; Keplin, B.; Pižl, V.; Tajovský, K.; Starý, J.; Lukešová, A.; Nováková, A.;
536 Balík, V. r.; Háněl, L.; Materna, J.; Düker, C.; Chalupský, J.; Rusek, J.; Heinkele, T., Soil biota
537 and upper soil layer development in two contrasting post-mining chronosequences. *Ecological*
538 *Engineering* **2001,** *17*, (2–3), 275-284.
539 64. Harrison, A. L.; Dipple, G. M.; Power, I. M.; Mayer, K. U., Influence of surface
540 passivation and water content on mineral reactions in unsaturated porous media: Implications for
541 brucite carbonation and CO_2 sequestration. *Geochimica et Cosmochimica Acta* **2015,** *148*, 477-
542 495.
543 65. Wilson, S. A.; Barker, S. S. L.; Dipple, G. M.; Atudorei, V., Isotopic disequilibrium
544 during uptake of atmospheric CO_2 into mine process waters: implications for CO_2 sequestration.
545 *Environmental Science & Technology* **2010,** *44*, 9522-9529.
546 66. Wilson, S. A.; Dipple, G. M.; Power, I. M.; Barker, S. L. L.; Fallon, S. J.; Southam, G.,
547 Subarctic weathering of mineral wastes provides a sink for atmospheric CO_2. *Environmental*
548 *Science & Technology* **2011,** *45*, 7727-7736.
549 67. Wilson, S. A.; Raudsepp, M.; Dipple, G. M., Quantifying carbon fixation in trace
550 minerals from processed kimberlite: A comparative study of quantitative methods using X-ray
551 powder diffraction data with applications to the Diavik Diamond Mine, Northwest Territories,
552 Canada. *Applied Geochemistry* **2009,** *24*, 2312-2331.
553 68. Mata, T. M.; Martins, A. A.; Caetano, N. S., Microalgae for biodiesel production and
554 other applications: A review. *Renewable and Sustainable Energy Reviews* **2010,** *14*, 217–232.
555 69. Google Earth, *Woodsreef, Barraba, NSW, Australia*, 7.1.1.1888; CNES/Astrium, 2014.
556
557

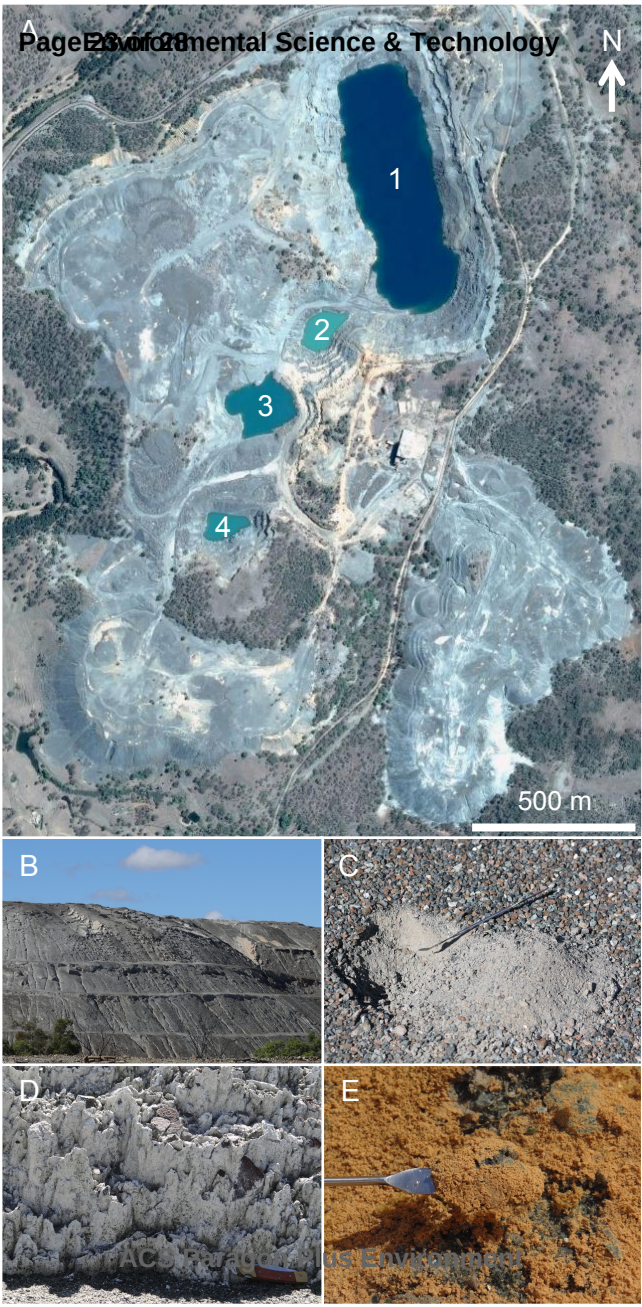

Figure 1

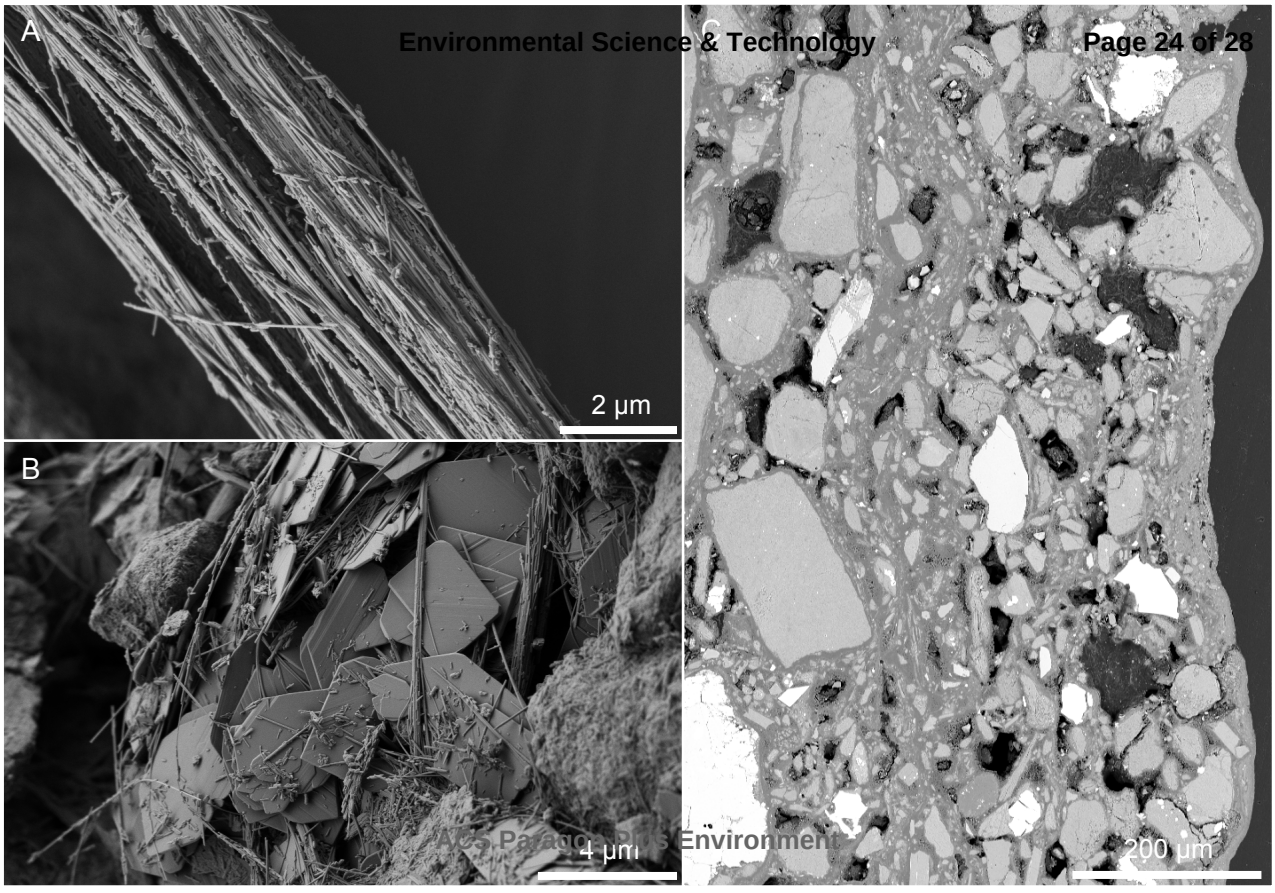

Figure 2

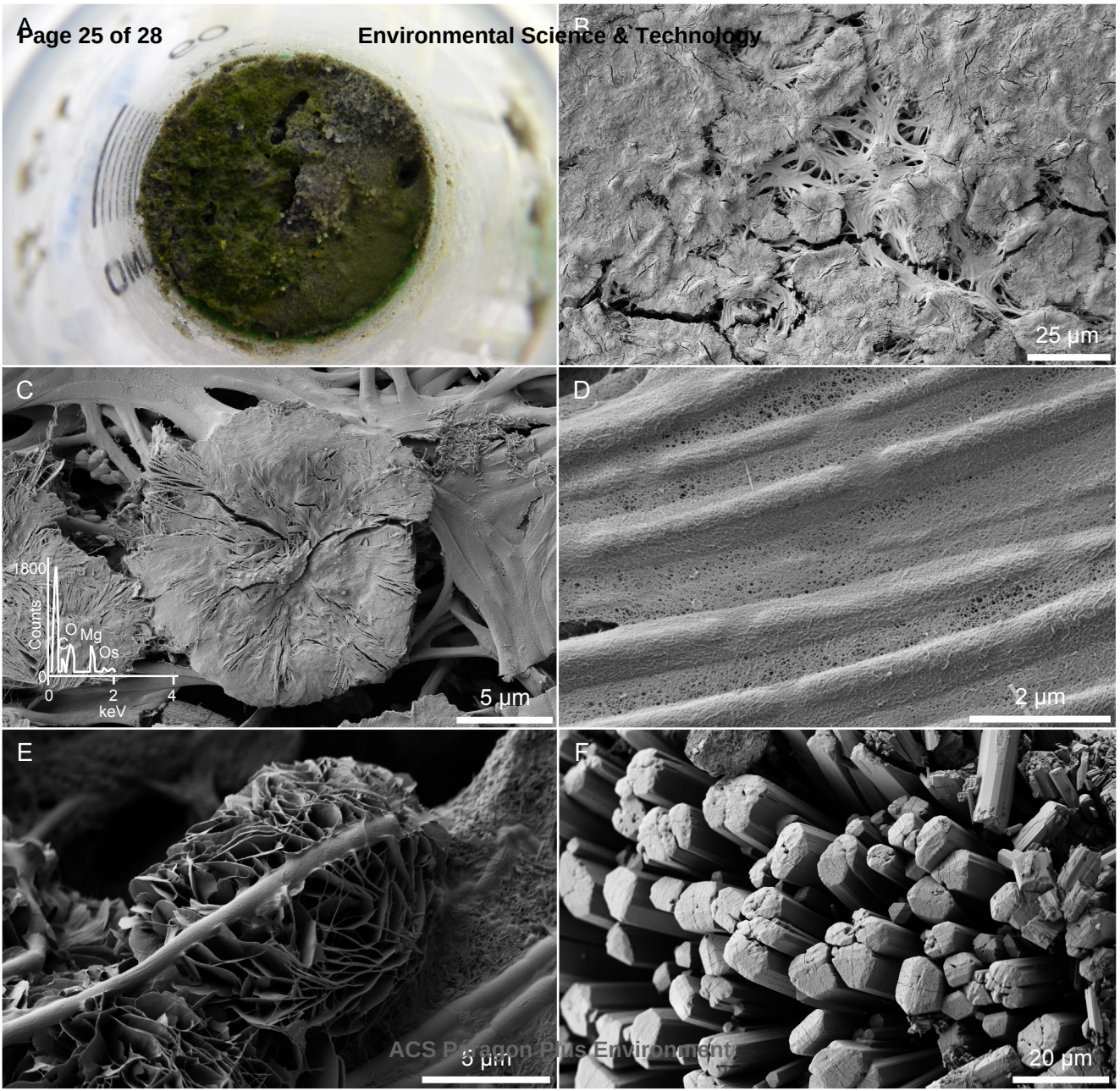

Figure 3

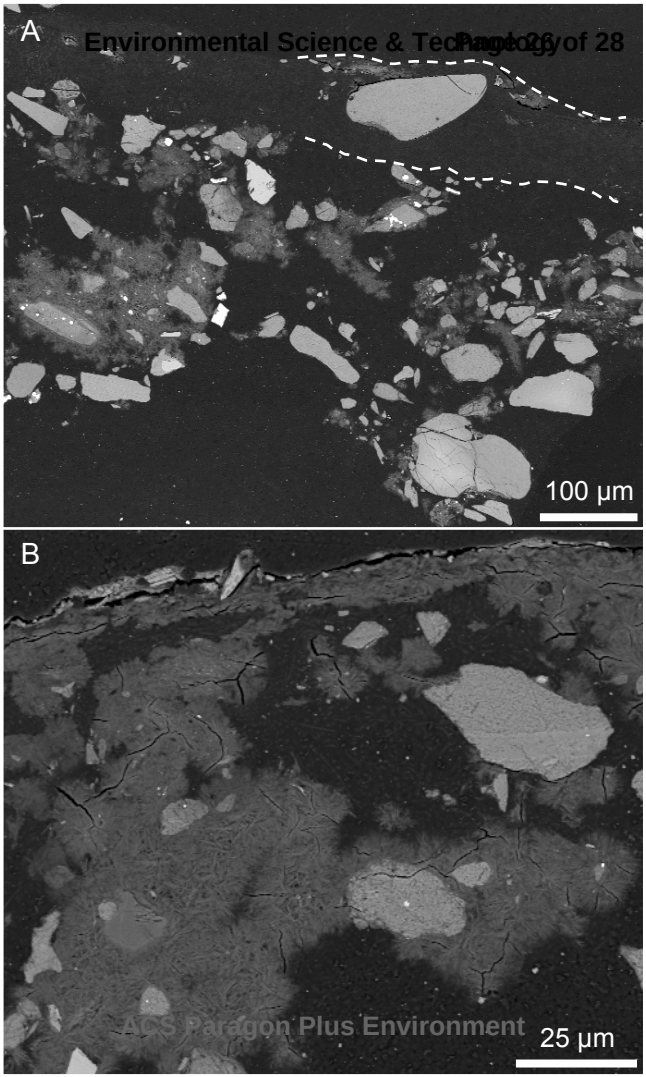

Figure 4

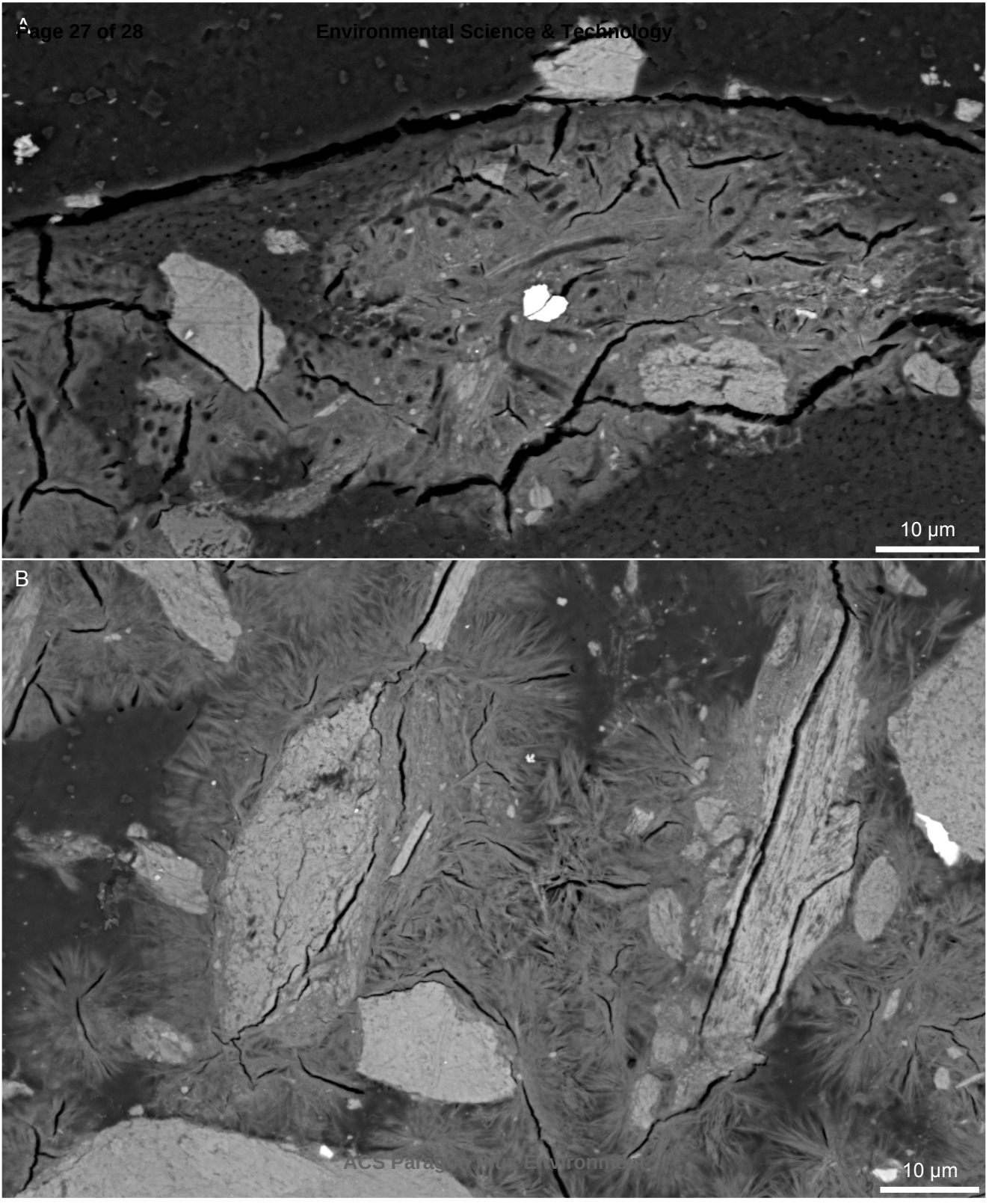

Figure 5